ACADEMIC PRESS

Available online at www.sciencedirect.com

SCIENCE DIRECT®

Clinical Immunology 108 (2003) 60–68

CLINICAL IMMUNOLOGY

www.elsevier.com/locate/yclim

Mutational effects on protein folding stability and antigenicity: the case of streptococcal pyrogenic exotoxin A

John H. Carra,[a,*] Brent C. Welcher,[a] Rowena D. Schokman,[a] Chella S. David,[b] and Sina Bavari[a,*]

[a] *United States Army Medical Research Institute of Infectious Diseases, Department of Cell Biology and Biochemistry, 1425 Porter Street, Frederick, MD 21702, USA*

[b] *Department of Immunology, Mayo Clinic, Rochester, MN 55905, USA*

Received 11 October 2002; accepted with revision 21 February 2003

Abstract

The influence of mutationally induced changes in protein folding on development of effective neutralizing antibodies during vaccination remains largely unexplored. In this study, we probed how mutational substitutions of streptococcal pyrogenic exotoxin A (SPEA), a model bacterial superantigen, affect native conformational stability and antigenicity. Stability changes for the toxin variants were determined using circular dichroism and fluorescence measurements, and scanning calorimetry. Self-association was assayed by dynamic light scattering. Inactivated SPEA proteins containing particular combinations of mutations elicited antibodies in HLA-DQ8 transgenic mice that neutralized SPEA superantigenicity in vitro, and protected animals from lethal toxin challenge. However, a highly destabilized cysteine-free mutant of SPEA did not provide effective immunity, nor did an irreversibly denatured version of an otherwise effective mutant protein. These results suggest that protein conformation plays a significant role in generating effective neutralizing antibodies to this toxin, and may be an important factor to consider in vaccine design.

Keywords: SPEA; Superantigen; Exotoxin; Vaccine; DSC; Circular dichroism; Protein folding

Introduction

Vaccines against protein toxins can often be generated from mutationally inactivated toxins produced in *E. coli.* However, the impact of these mutations on conformational stability, as it relates to effective antigenicity, remains relatively unexplored. Consequently, this study focused on examining the impact of mutant residues on protein folding, and subsequent vaccine design, against streptococcal pyrogenic exotoxin A (SPEA) [1]. SPEA[1] is a major virulence factor released by *Streptococcus pyogenes* and is associated with scarlet fever and severe invasive infections [1–4].

SPEA belongs to a class of toxins that are collectively referred to as superantigens. These proteins possess the ability to simultaneously bind to the major histocompatibility complex (MHC), outside of the peptide antigen presentation groove, and the Vβ chain of T-cell receptors (TCR). The resulting unrestricted interactions between T cells and antigen-presenting cells lead to the activation of a large population of T cells, as well as the hyperproduction of inflammatory cytokines. Subsequent physiological consequences include rash, hypotension, and, in severe cases, multiple organ failure. The continuing public health threat posed by streptococcal infections and the emergence of antibiotic-resistant strains of this species of bacteria indicate the need for a protective vaccine [5]. In accordance with this goal, efforts to develop a vaccine against SPEA from a recombinant, mutationally inactivated toxin mandate a bet-

* Corresponding author. Fax: +1-301-619-2348.

E-mail addresses: john.carra@det.amedd.army.mil (J.H. Carra), sina.bavari@det.amedd.army.mil (S. Bavari).

[1] Abbreviations used: SPEA, streptococcal pyrogenic exotoxin A; SEA, staphylococcal enterotoxin A; CD, circular dichroism; DSC, differential scanning calorimetry; DLS, dynamic light scattering; TCR, T-cell receptor; HLA, human leukocyte antigen; MHC, major hostocompatibility complex; PBMC, peripheral blood mononucleocytes; T_t, transition temperature; SAg, superantigen.

1521-6616/03/$ – see front matter © 2003 Elsevier Science (USA). All rights reserved.
doi:10.1016/S1521-6616(03)00058-5

Report Documentation Page

Form Approved
OMB No. 0704-0188

1. REPORT DATE	2. REPORT TYPE	3. DATES COVERED
21 FEB 2003	**N/A**	**-**

4. TITLE AND SUBTITLE	5a. CONTRACT NUMBER
Mutational effects on protein folding stability and antigenicity: the case of streptococcal pyrogenic exotoxin A, Clinical Immunology 108:60 - 69	5b. GRANT NUMBER
	5c. PROGRAM ELEMENT NUMBER
6. AUTHOR(S)	5d. PROJECT NUMBER
Carra, JH Welcher, BC Schokman, RD David, CS Bavari, S	5e. TASK NUMBER
	5f. WORK UNIT NUMBER
7. PERFORMING ORGANIZATION NAME(S) AND ADDRESS(ES)	8. PERFORMING ORGANIZATION REPORT NUMBER
United States Army Medical Research Institute of Infectious Diseases, Fort Detrick, MD	
9. SPONSORING/MONITORING AGENCY NAME(S) AND ADDRESS(ES)	10. SPONSOR/MONITOR'S ACRONYM(S)
	11. SPONSOR/MONITOR'S REPORT NUMBER(S)

12. DISTRIBUTION/AVAILABILITY STATEMENT

Approved for public release, distribution unlimited

13. SUPPLEMENTARY NOTES

The original document contains color images.

14. ABSTRACT

The influence of mutationally induced changes in protein folding on development of effective neutralizing antibodies during vaccination remains largely unexplored. In this study, we probed how mutational substitutions of streptococcal pyrogenic exotoxin A (SPEA), a model bacterial superantigen, affect native conformational stability and antigenicity. Stability changes for the toxin variants were determined using circular dichroism and fluorescence measurements, and scanning calorimetry. Self-association was assayed by dynamic light scattering. Inactivated SPEA proteins containing particular combinations of mutations elicited antibodies in HLA-DQ8 transgenic mice that neutralized SPEA superantigenicity in vitro, and protected animals from lethal toxin challenge. However, a highly destabilized cysteine-free mutant of SPEA did not provide effective immunity, nor did an irreversibly denatured version of an otherwise effective mutant protein. These results suggest that protein conformation plays a significant role in generating effective neutralizing antibodies to this toxin, and may be an important factor to consider in vaccine design.

15. SUBJECT TERMS

superantigens, exotoxin, vaccine, circular dichroism, protein folding, laboratory animals, mice

16. SECURITY CLASSIFICATION OF:			17. LIMITATION OF ABSTRACT	18. NUMBER OF PAGES	19a. NAME OF RESPONSIBLE PERSON
a. REPORT	b. ABSTRACT	c. THIS PAGE			
unclassified	**unclassified**	**unclassified**	**SAR**	**9**	

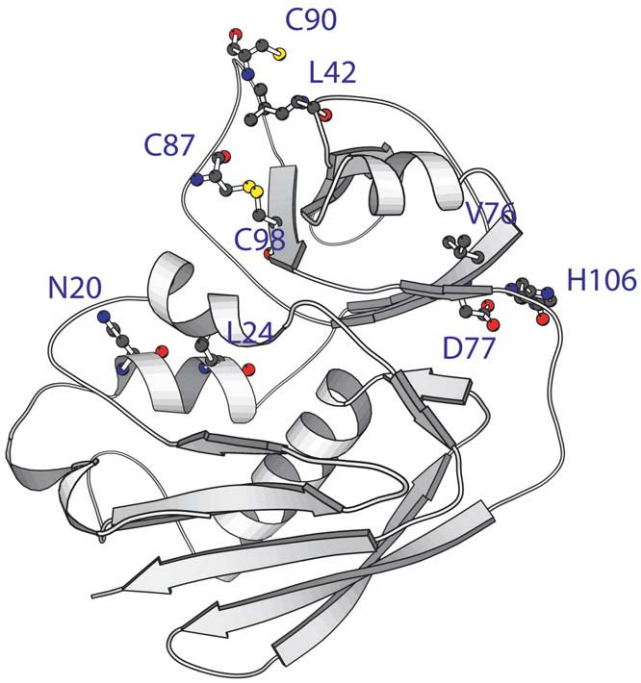

Fig. 1. Molscript[15] diagram of SPEA. Positions where residue substitutions were made are indicated in ball-and-stick representation. Coordinates (1B1Z.pdb) from Papageorgiou et al. [6].

ter understanding of the relationships between structure, function, and protective antigenicity for this protein.

The X-ray crystal structure of SPEA has been solved at 2.6-Å resolution [6], revealing N- and C-terminal subdomains, and a surface loop constrained by a disulfide bond between residues C87 and C98. In addition, another cysteine (located at position 90) is also inside this loop (Fig. 1). Modeling and mutational analyses [7,8] have predicted that the disulfide loop is important for interactions with both TCR and MHC in the ternary SPEA–TCR–MHC complex. A recent cocrystal structure of the C90S mutant of SPEA with a mouse TCR β chain [9] confirmed the involvement of loop residues in binding to TCR.

Chromatographic separation of recombinantly produced SPEA protein isolated at pH 7.9 revealed the presence of both monomer and dimer species, leading Papageorgiou et al. [6] to speculate that residue C90 in one toxin monomer forms a disulfide bond to the C90 of another SPEA molecule. We confirm here using dynamic light scattering measurements on a C90A mutant protein at pH 7.0 that this residue does indeed form such a disulfide-linked dimer. The SPEA protein examined by Papageorgiou and colleagues was isolated at pH 5.7 to inhibit disulfide formation and crystallized in an asymmetric unit of a tetramer, which has raised speculation that this toxin may function as such in vivo.

A zinc-binding site on SPEA at the locus of residues D77 and H106 has also been identified and confirmed by several groups [6,9–11]. Baker et al. [11] found that residues E33, D77, H106, and H110 ligate zinc ion with a K_D of 2.3 μM. The significance of zinc for physiological function of SPEA is not yet clear. However, Hartwig and Fleischer (1993) [12] found that a SPEA D77A mutant protein was unable to bind class II MHC on the surface of antigen-presenting cells, while Baker et al. [11] suggested that the zinc site is a potential second MHC-binding locus, as judged from molecular modeling.

Other studies have identified additional SPEA mutations and residues that are important for the activity of this toxin. The naturally occurring substitution V76I, known as the SPEA3 allele [13], has been shown to possess an eightfold higher affinity for HLA-DQ than SPEA1 [7,8]—even though it is not located at the predicted MHC-binding surface. Residues N20 [5,14] and L24 have been predicted to be at or near the TCR interaction surface, while residue L42 is believed to be located in the SPEA contact site for MHC class II molecules [7,8]. Residue N20 is observed to contact the TCR β chain in the structure of Sundberg et al. (2002) [9].

The objective of this study was to determine the effects of previously studied mutations on SPEA stability and test for a correlation with changes in the effectiveness of neutralizing antibodies elicited during vaccination. Knowledge of the significance of protein folding vs antigenicity gained from studying model systems such as SPEA may be valuable in designing more robust vaccines against bacterial SAgs and other proteins.

Materials and methods

1. Mutagenesis and protein purification

For expression, the SpeA1 allele gene [13] was cloned into the T7 polymerase vector pET24b (Novagen). BL21(DE3) Gold (Novagen) *E. coli* cultures were grown in shaker flasks at 30°C for 16 h, without IPTG induction, which was found to be unnecessary. Cells were lysed with lysozyme and lysates fractionated using 30% ammonium sulfate. The pellet was discarded, and the supernatant precipitated with 60% ammonium sulfate. This pellet was resuspended in buffer A (20 mM NaOAc, pH 5.0) and dialyzed overnight against 2 L of the same buffer, with one change of solution. Precipitated material was removed by centrifugation, and the cleared supernatant applied to a Sepharose-SP (Pharmacia) cation exchange column. The protein obtained by salt gradient elution was dialyzed against 2 L of buffer A and reapplied to the same column. After these steps, the isolated protein was judged to be >99% pure by SDS–gel electrophoresis. Yields were typically 10–50 mg/L of *E. coli* culture. Protein concentrations were measured using UV absorbance at 277 nm, with an A_{277} value of 0.870 for a 1 mg/mL solution (25,789 MW_r), determined by the method of Gill and von Hippel [16]. Measurement of endotoxin content using a limulus amebo-

cyte assay (Bio-Whittaker) indicated less than 0.1 μ/mg of protein.

2. Circular dichroism and fluorescence measurements

Circular dichroism and fluorescence were measured using a Jasco-810 spectropolarimeter equipped with an automatic titrator, a temperature controller, and a fluorescence detector. Far-UV wavelength spectra were collected at 25°C in a 1-mm pathlength rectangular cell, at protein concentrations close to 0.4 mg/mL in 20 mM NaOAc, pH 4.0. Data were not smoothed.

For guanidine–HCl titration experiments, a cell with four polished sides (Starna Cells) was used with a 0.5-cm pathlength in the direction of the circular dichroism measurement, and a 1-cm path for fluorescence detection at right angles. The buffer was 10 mM Na phosphate, pH 7.0. An automatic titrator was employed to make 40 injections of 40 μL each of 8.2 M guanidine–HCl into 1.2 mL of protein solution over 2.5 h at 25°C. The concentration of guanidine–HCl solutions was measured using a refractometer [17]. Measurements were of circular dichroism at 225 nm and total fluorescence above 305 nm, with excitement at 280 nm to maximize signal. Analysis of protein samples after removal of denaturant by dialysis showed that guanidine–HCl-induced unfolding of SPEA at 25°C was a reversible process, allowing the application of equilibrium thermodynamics. Heat-induced unfolding was effectively irreversible as measured by CD or DSC.

3. Nonlinear regression

Denaturation curves monitored by CD were fit globally using a nonlinear regression routine implemented with the program NLREG (Phillip Sherrod, author). The Gibbs free energy change of unfolding in water [18] was obtained from the following:

$$\Delta G = \Delta G_{H_2O} - m * [\text{den}] .$$

The m value (dependence of ΔG on denaturant concentration in kJ mol^{-1} M^{-1}) was a fitted parameter held in common across the data set, while ΔG_{H_2O} ($= -\Delta G_{fold}$) values were fitted to all curves simultaneously. For the curves of Fig. 2B, the CD and fluorescence signals as a function of guanidine–HCl were fit simultaneously, while the ΔG_{H_2O} value was allowed to vary as a parameter in common for the two curves and m was set to be 6.9 kJ mol^{-1} M^{-1}.

4. Dynamic light scattering

A Dyna-Pro MS800 instrument (Protein Solutions, Inc.) was used to make right-angle dynamic laser-light scattering measurements on protein solutions (10 mM Na phosphate, pH 7.0) in a 12-μL cuvette at 25°C. Twenty measurements were made, data with poor fits to the correlation function were discarded, and the hydrodynamic radius (R_H) was obtained as an average. Protein molecular weights were estimated using the standard curve for small globular proteins contained in the Dynamics software package. Samples were allowed to equilibrate at room temperature for 1 day prior to measurement, and were injected through a 0.02-μm filter directly into the cuvette.

5. Differential scanning calorimetry

Scanning calorimetry on SPEA proteins was performed using a Nano-2 instrument [19] from Calorimetry Sciences Corporation, with a scan rate of 1 K min^{-1}, in 25 mM NaOAc, pH 4.0. Unfolding curves were irreversible as judged by second scanning of samples, and showed a significant scan rate dependence, precluding detailed thermodynamic analysis. Melting of the proteins at pH 7.0, including cysteine-free mutants, resulted in precipitation upon unfolding. Use of low pH avoided protein precipitation, but did not allow reversibility of unfolding.

6. Transgenic mouse procedures

HLA-DQ8/human CD4+ transgenic mice were created by microinjecting DNA fragments into embryos from C57BL/6 mice, as previously described [20]. Research was conducted in compliance with the Animal Welfare Act and other Federal statutes and regulations relating to animals and experiments involving animals, and adheres to principles stated in the *Guide for the Care and Use of Laboratory Animals,* National Research Council, 1996. The facility where this research was conducted is fully accredited by the Association for Assessment and Accreditation of Laboratory Animal Care International.

Mice were injected intraperitoneally (ip) with 10 μg of mutant SPEA protein in 100 μL of Ribi's adjuvant (Ribi Immunochem Research, Hamilton, MT) or with adjuvant alone. Mice were boosted at 2 and 4 weeks in the same manner as described for the initial injection. Serum was collected from tail veins 1 week after the last vaccination. Mice were challenged 2 weeks after the third vaccination with 10 μg of wild-type SPEA, and survival was scored over 7 days.

Fig. 2. (A) Global fitting of guanidine hydrochloride-induced denaturation of SPEA proteins, monitored by circular dichroism at 225 nm. Data are in symbols, fitted results in lines. (B) Denaturation of SPEA C87A+C90A+C98A monitored simultaneously by CD at 225 nm and total fluorescence over 305 nm. Dashed lines indicate pre- and posttransitional baseline assignments.

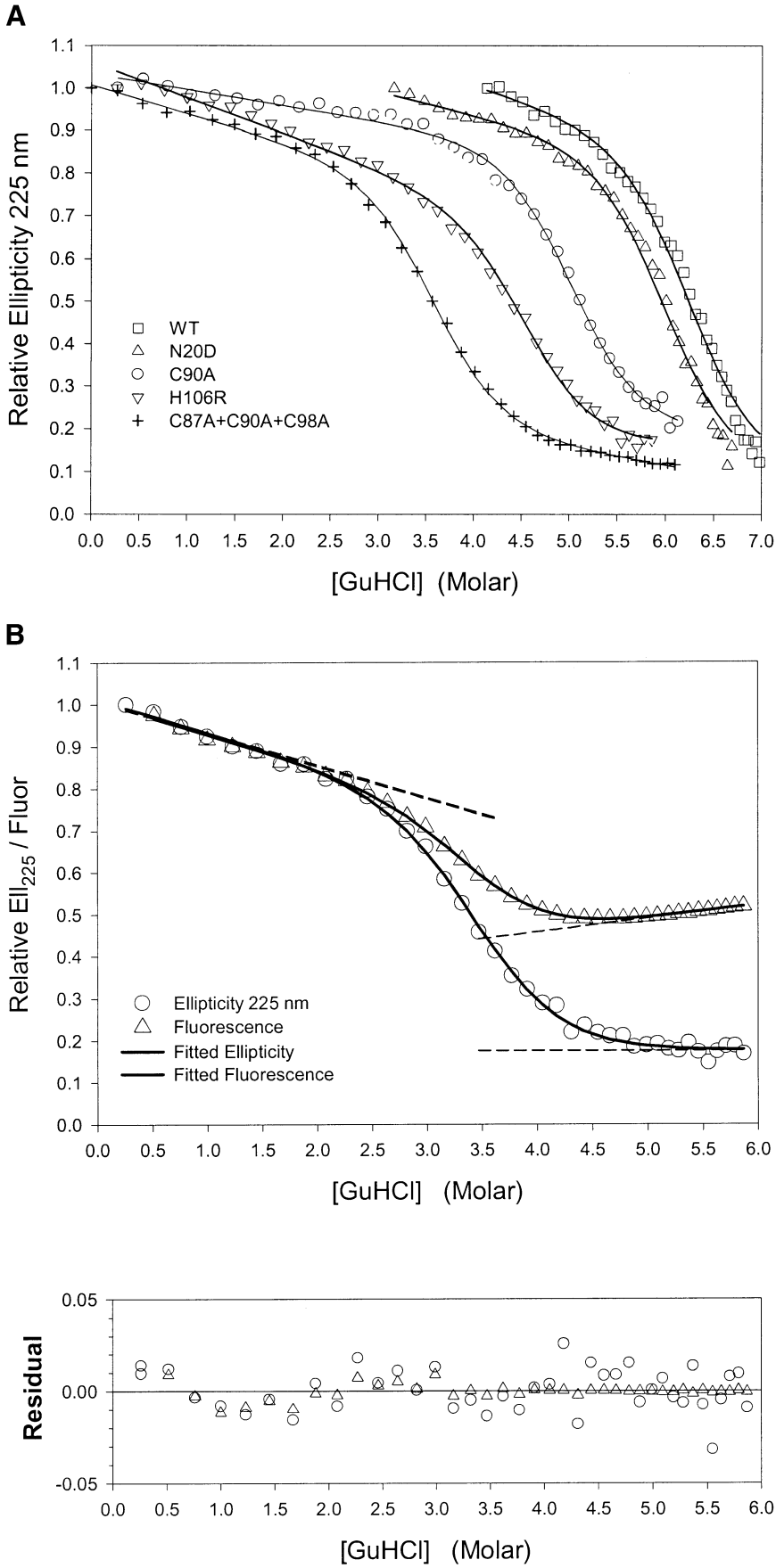
A
Relative Ellipticity 225 nm
WT
N20D
C90A
H106R
C87A+C90A+C98A
[GuHCl] (Molar)
B
Relative Ell225 / Fluor
Ellipticity 225 nm
Fluorescence
Fitted Ellipticity
Fitted Fluorescence
[GuHCl] (Molar)
Residual
[GuHCl] (Molar)

7. Serum antibody and T-cell stimulation assays

Wells of microtiter plates were coated with 1 μg/well of wild-type (wt) SPEA in 100 μL of PBS (4°C, 24 h); 100 μl of mouse sera diluted in PBS plus 0.02% casein was added to duplicate wells and incubated (37°C, 1 h). Bound antibody was detected by incubation (37°C, 1 h) with goat anti-mouse conjugated to horseradish peroxidase followed by the addition of 100 μl 3,3′,5,5′-tetramethyl-benzidine (TMB) peroxidase substrate. The mean of duplicate optical densities (absorbance at 650 nm) of each group was obtained.

To assay for neutralization of SPEA activity by serum antibodies, we used the T-lymphocyte proliferation assay [21]. To demonstrate SPEA-specific T-cell inhibition by pooled mouse sera obtained from vaccinated or control mice, sera were incubated (1 h/37°C) with a various doses of SPEA (20 or 200 ng/ml). The mixture was added to donor mononuclear cells obtained from an unvaccinated HLA-DQ8 transgenic mouse spleen and the amount of [^{3}H]thymidine incorporation (cpm) was measured by a liquid scintillation counter. All cultures were performed in triplicate. The data are presented as percentage of SPEA inhibition of T-cell proliferation by serum from experimental, where inhibition = 100 − [(cpm for sera from vaccinated mice in presence of SPEA)/(cpm for pooled sera from unvaccinated mice in presence of SPEA) × 100].

Results

Thermodynamics of wild-type and mutant SPEA proteins

The stability of a protein's structure can be determined by monitoring spectral changes associated with unfolding induced by denaturants, and extrapolating these measurements back to zero denaturant concentration (reviewed in Pace and Shaw [22]). Using guanidine hydrochloride as the denaturant, and circular dichroism measurements, we determined mutational effects on the Gibbs free energy of protein folding (ΔG_{fold}) for SPEA variants (Fig. 2A, Table 1). The individual ΔG_{fold} values for each mutant were derived from global nonlinear regression analysis of the CD data.

In the absence of evidence of deviations from two-state behavior for the various mutant proteins, a two-state model was adapted. A single common *m* parameter, which represents the sensitivity of ΔG_{fold} to guanidine–HCl concentration, was used. The method of global fitting to a common *m* value avoids some uncertainties introduced by varying pre- and posttransitional baseline assignments when fitting is done independently across a set of unfolding curves. The results obtained for $\Delta\Delta G_{fold}$ (Table 1) are also in agreement with the order of corresponding C_m values (i.e., denaturant concentrations of half-unfolding).

A value for *m* of 6.9 kJ mol^{-1} M^{-1} was obtained for the examined mutants. Success in achieving a good fit across the dataset with this approach supports the assumption that *m* values and the cooperativity of folding are not greatly affected by these mutational changes. The mutational effects are not additive, which may be due to subtle readjustments in structure resulting from the introduction of each mutation. Errors in ΔG_{fold} are estimated to be ±10%, and result mainly from uncertainties in baseline assignments.

Table 1
Stabilities of mutant SPEA proteins

Protein	ΔG_{fold}[a]	$\Delta\Delta G$[b]	C_m[c]
wt (SpeA1)	−44	—	6.3
V76I	−36	8	5.2
L42A	−46	−2	6.6
N20D	−42	2	6.0
D77A	−36	8	5.2
H106R	−32	12	4.6
L24A	−35	9	5.0
C90A	−34	10	4.9
L42A + N20D	−34	10	4.9
L42A + N20D + C90A	−33	11	4.7
L42A + N20D + L24A	−35	9	5.1
L42A + N20D + D77A	−36	8	5.2
C87A + C90A + C98A	−21	23	3.2

[a] Gibbs free energy change of protein folding ΔG in kJ mol^{-1}.
[b] Difference in ΔG between wt SPEA and mutant proteins.
[c] Midpoint concentration of guanidine–HCl induced denaturation (molar).

Fig. 2B shows the results of global fitting of simultaneously acquired CD and total fluorescence emission data as a function of guanidine–HCl concentration for the triple mutant protein C87A + C90A + C98A. *m* was set to the same value as that obtained from the global fit of all proteins. The residuals of the fit show only a small degree of autocorrelation, indicating minimal apparent deviation from the model. The agreement of these two different probes of protein structure supports our assumption that denaturation of SPEA is essentially a two-state process, although absolute proof cannot be obtained by this method. For the mutants unfolding at higher denaturant concentrations, fluorescence was not as useful a probe due to the quenching of native state fluorescence by guanidine–HCl.

The large ΔΔG of 23 kJ mol^{-1} for the C87A + C90A + C98A triple mutant (Table 1) indicates that the disulfide bond between residues 87 and 98 has a major stabilizing effect on the protein's structure. The standard deviation in ΔG_{fold} of repeated measurements of this mutant protein was 0.5 kJ mol^{-1}.

The far-UV CD spectra of the mutant proteins (data not shown) revealed no significant differences in secondary structure content compared to wt SPEA, except in one case, that of the triple mutant C87A + C90A + C98A. This mutant has slightly more negative ellipticity at 210 nm than wild-type (−5492 vs −3920 deg cm^2 dmol^{-1}) and a zero ellipticity crossover point of 205 nm, vs 204 nm for wild-

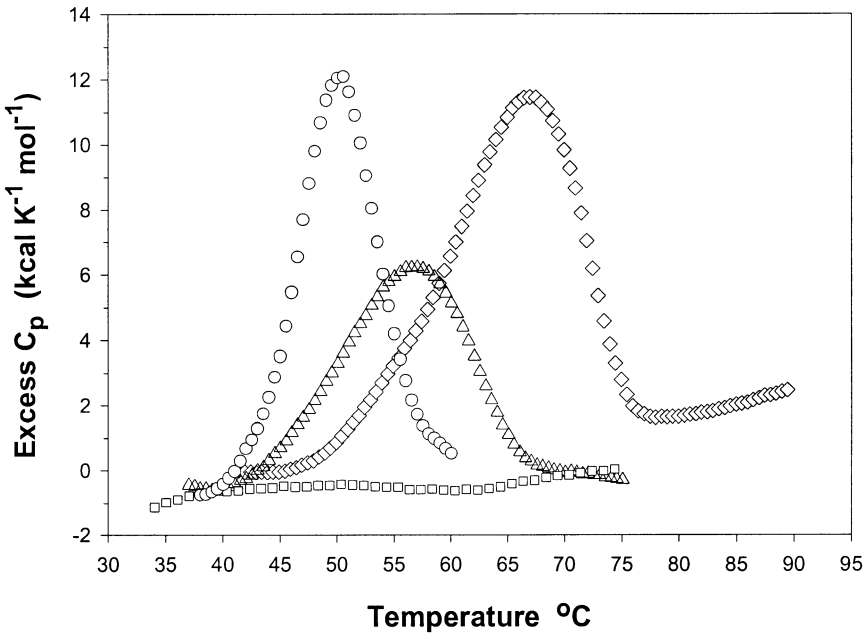

Fig. 3. Differential scanning calorimetry on wt and mutant SPEA proteins. C87A+C90A+C98A (circles), L42A+N20D+D77A first scan (triangles) and second scan (squares), wt (diamonds).

type SPEA. This result is consistent with a small increase in conformational disorder caused by elimination of the disulfide bond between C87 and C98. The C90A mutant, in contrast, had a spectrum very similar to that of the wt protein, indicating that the aforementioned conformational changes result from the loss of the C87-C98 bond.

Fig. 3 shows the results of scanning calorimetry experiments on wild-type SPEA, and the L42A + N20D + D77A and C87A + C90A + C98A mutants. All transitions were found to be completely irreversible, as revealed by a second scanning of samples, which precluded the use of detailed thermodynamic analysis based on the assumption of equilibrium. The curve for SPEA showed an obvious asymmetry, which often results from exothermic effects associated with irreversibility. Similarly, the curve for L42A + N20D + D77A is also somewhat asymmetric. By contrast, C87A + C90A + C98A yielded a symmetric curve, without an obvious exotherm following denaturation. This may result from either the absence of heat-induced disulfide cross-linking or lesser hydrophobic associations of the denatured state at a lower transition temperature. The calorimetric enthalpy change ΔH_{cal} of C87A + C90A + C98A at its transition temperature (T_t) of 50.3°C was 410 kJ/mol. Exothermic effects present for the other proteins prevented determination of accurate ΔH and T_t values. Although both of the combination mutants were greatly destabilized relative to the wt, both existed substantially in the native state at 37°C, under the pH 4.0 conditions utilized here and at pH 7.0 (not shown). In general, the order of mutant stabilities, as judged by the appearance of the melting peaks, was the same as that obtained during guanidine–HCl denaturation.

Dimerization

Association of the wild-type (SPEA1) and mutant SPEA proteins was assayed by dynamic light scattering, which is capable of detecting oligomerization of small globular proteins. Table 2 gives the hydrodynamic radius (R_H) and the calculated molecular weight of the protein species. Wild-

Table 2
Association observed by dynamic light scattering

Protein	R_H[a]	MW[b]	[Protein][c]
wt	3.27	53.8	1.72
wt	3.30	55.0	0.86
wt	3.11	47.9	0.43
wt	3.16	49.7	0.22
wt + 0.1 mM $ZnCl_2$	3.16	49.7	1.72
wt + 1 mM EDTA	3.11	47.9	1.72
wt + 1 mM DTT	2.66	33.2	1.76
V76I	2.97	43.0	0.86
L42A	3.36	57.4	1.80
N20D	3.06	46.1	1.38
D77A	2.98	43.3	0.62
H106R	3.12	48.2	1.28
L24A	3.55	65.3	0.75
C90A	2.42	26.6	1.94
L42A + N20D	2.93	41.6	0.84
L42A + N20D + D77A	2.82	38.1	1.30
L42A + N20D + L24A	3.11	47.9	1.11
L42A + N20D + C90A	2.39	25.9	1.24
C87A + C90A + C98A	2.45	27.4	1.15

[a] Hydrodynamic radius R_H in nm.
[b] Apparent molecular weight of the protein species calculated from R_H.
[c] Protein concentration in mg/mL.

type SPEA in these preparations was found to existed predominantly as a dimer, having an apparent MW_r of 53.8×10^3. Hence, for SPEA at 25,789 MW_r, a value of 25.8×10^3 corresponds to a monomer and a value of 51.6×10^3 to a dimer. Furthermore, SPEA self-association was not dependent on either the protein concentration between the range 0.22 to 1.72 mg/mL or the addition of 0.1 mM $ZnCl_2$ or 1 mM EDTA. Unlike dimerization of staphylococcal enterotoxin D [23], SPEA dimerization was not induced by zinc.

Incubation of SPEA with the reducing agent dithiothreitol at 1 mM decreased the protein's average apparent relative molecular weight from 53.8×10^3 to 33.2×10^3. Of the mutant SPEA proteins assayed, only the C90A mutant, and combinations thereof, resulted in complete elimination of the dimer species. These results strongly indicate that the observed protein dimer was formed by an intermolecular disulfide bond between the C90 residues of two separate SPEA molecules, as was previously proposed by Papageorgiou et al. [6].

Vaccine testing in transgenic mouse model

In order to determine the effects of amino acid mutations on the protein's protective antigenicity, we used a transgenic mouse model bearing the susceptible HLA alleles for SPEA toxicity [24]. This transgenic murine model expresses HLA-DQ8 and human CD4, and succumbs to SPEA-induced lethal shock without additional sensitization. Importantly, this transgenic model allowed for the examination of the efficacy of vaccine candidates against SPEA in the context of HLA.

Residue L42 lies within a hydrophobic loop and has been identified as one of the key residues that SPEA and other bacterial superantigens use to interact with class II MHC molecules [25]. Mutation of SPEA L42 substantially decreases toxicity [7,8], which is a necessary prerequisite for vaccination without lethality. Therefore, for testing immunogenicity we concentrated our efforts on using this mutation alone and in combination with other substitutions.

The HLA-DQ8 mice were injected with 10 μg of the attenuated SPEA mixed with adjuvant, or adjuvant only, every 14 days. The animals were examined postvaccination individually for: (1) antibody titers against wt SPEA; (2) the ability of serum taken at the time of challenge to inhibit SPEA-induced proliferation in T cells in vitro; and (3) survival after challenge. After the first boost, serum was obtained and antibody titers against SPEA were determined for each of the transgenic mice. All mice vaccinated with SPEA protein variants developed detectable titers against SPEA. Mice vaccinated with SPEA C87A + C90A + C98A produced the lowest titers after the first boost. After the third vaccination, all mice elicited higher antibody titers; however, mice injected with SPEA C87A + C90A + C98A again produced the lowest titers. Control mice injected with adjuvant only had no serum antibody responses against SPEA.

Table 3
Mutational effects on SPEA vaccine efficacy

Vaccine	Titers after vaccination[a]		Inhibition of T-cell responses[b]	Survival[c] live/total
	Second	Third		
L42A	$>10^4$	$>10^5$	80	6/7 (0.0035)
L42A+N20D	$>10^4$	$>10^5$	75	7/7 (0.0002)
L42A+N20D+D77A	$>10^4$	$>10^5$	74	7/7 (0.0002)
L42A+N20D+L24A	$>10^4$	$>10^5$	79	7/7 (0.0002)
L42A+N20D+C90A	$>10^4$	$>10^5$	90	6/7 (0.0035)
C87A+C90A+C98A	10	10^3	40	1/7 (0.7961)
C90A	$>10^4$	$>10^4$	65	6/7 (0.0035)
Heat-denatured				
L42A+N20D+D77A	$>10^4$	$>10^4$	47	1/7 (0.7961)
Adjuvant	10	10	0	0/7

[a] Mice were vaccinated ip and boosted at 2 and 4 weeks. On the day of the second vaccination and 10 days after the last vaccination, mice were bled and serum titers against SPEA determined. Data are presented as reciprocal serum dilution resulting in OD reading twice above negative controls (ELISA wells containing either no toxin or no primary antibody).

[b] SPEA (20 ng/mL) and sera that was obtained 10 days after the last vaccination were preincubated before adding to splenic mononuclear cells. The data are presented as percentage of SPEA stimulation, as described under Materials and Methods. Standard error of the mean of triplicate wells were $< 10\%$ for calculated values.

[c] Mice were challenged with 10 μg/mouse of SPEA (approximately 10 LD_{50}) 2 weeks after the final boost and lethality was recorded 7 days after the challenge dose. ρ values are shown in parenthesis and were obtained by one-tailed Fisher's exact test with a bootstrap adjustment for multiple comparisons to the adjuvant control group.

To determine if the vaccination elicited serum antibodies were capable of preventing SPEA-induced T-cell proliferation, and to further characterize any differences in SPEA mutant vaccines that would not have otherwise been observed in the survival data, the neutralizing ability of the vaccinee's serum in a T-cell proliferation assay was analyzed. Wild-type SPEA was incubated with pooled sera obtained from mice immunized with SPEA vaccine adjuvant only. The mixture of toxin and sera was added to splenic T cells obtained from naïve HLA-DQ8 transgenic mice, and SPEA-induced T-cell proliferation was measured. Sera obtained from SPEA C87A + C90A + C98A and heat-denatured SPEA L42A + N20D + D77A vaccinated mice displayed the lowest neutralization ability (Table 3), reducing T-cell proliferation by less than 50%. In contrast, sera obtained from other SPEA constructs showed inhibited T-cell proliferation up to 90%. This indicated that select SPEA mutant vaccines elicited substantial amounts of antibodies that neutralized SPEA associated superantigenicity.

To evaluate if the immune responses against the different SPEA mutant proteins translated into protection in vivo, 2 weeks after the third vaccination, the treated transgenic mice were challenged with 10 μg of wt SPEA, and survival was scored after 7 days (Table 3). By 48 h, all mice that were vaccinated with adjuvant only had died. In contrast, mice vaccinated with SPEA L42A, SPEA C87A + C90A +

C98A, or heat-denatured SPEA L42A + N20D + D77A displayed partial protection as judged by survival of some individuals. However, these survivors were all visibly stressed. All of the transgenic mice vaccinated with other SPEA constructs survived the challenge with no visible effect. These data suggest that changes in structural content and stability of the protein antigen may have dramatic effects on vaccine efficacy.

Discussion

To gain a better understanding of the significance of particular residues of SPEA for folding and immunogenicity, select mutational variants were examined. With the exception of mutant L42A, which was slightly more stable than wt SPEA, each mutational substitution had some degree of destabilizing effect on protein folding (Table 1). Proteins containing combinations of inactivating mutations were generated as candidates for vaccines and tested in a HLA-DQ8 transgenic mouse model for the production of neutralizing antibodies capable of protecting the animals from challenge with wild-type SPEA toxin. The most destabilized mutant (C87A + C90A + C98A) provided the mice with very poor protection. These results indicate that the disulfide loop region of SPEA is critical to the stability of the protein's tertiary fold, and suggest that its stabilizing effect on the SPEA structure is necessary for eliciting neutralizing antibody responses.

Primary sequence changes in the mutant may also contribute directly to the loss of neutralizing antigenicity, and cannot be ruled out by this type of experiment. However, another otherwise effective vaccine candidate protein, L42A + N20D + D77A, when irreversibly heat-denatured was only partially protective, suggesting that folding of the protein, and not just its primary sequence, is important for effective antigenicity. Antibodies raised to the denatured protein may be specific to that conformation, and therefore ineffective in providing protection against toxin challenge.

These studies also revealed that SPEA protein folding can be globally destabilized by at least as much as 8 kJ/mol (L42A + N20D + D77A), and still retain the ability to function as an effective antigen. However, the mutant C87A + C90A + C98A, which was destabilized by 23 kJ/mol, and the heat-denatured L42A + N20D + D77A were ineffective. Larger alterations in stability of the native state may be associated with changes in conformation at either the local or the global level that could affect antigenicity. In particular, the disulfide loop region appears to be critical to the activity of SAgs [26], and therefore may represent a critically important epitope.

SPEA mutant L42A + N20D + D77A displayed no measurable mitogenicity on human PBMC in vitro, and did not bind to MHC expressed on the surface of LG2 cells (not shown), making it a promising vaccine candidate. To decrease the chances that this protein will have any superantigenicity in vivo, the binding sites for all three factors known to bind SPEA have been mutated: TCR (N20D), MHC (L42A), and Zn^{2+} (D77A). Other combinations of mutations in SPEA were also found by Roggiani et al. [5] to provide good protection, using a rabbit model and potentiation with endotoxin.

Although results from this investigation indicated that SPEA prepared from *E. coli* exists at least partially as a disulfide-linked dimer (between C90A residues on separate molecules), dimerization was not critical to antigenicity, as revealed by the strong protection to challenge provided by the mutant C90A (Table 3). The similar dependency on guanidine–HCl concentration for denaturation of the monomeric mutants C90A and C87A + C90A + C98A, versus the other partially dimeric proteins, suggests that the dimer does not have a significantly greater folding stability than the monomer. Such a difference in stability between the monomeric and dimeric forms would have produced more biphasic curves, which it did not. We therefore considered the proteins to have a monomeric cooperative unit for the purposes of calculations.

The influence of protein structure on antigenicity is a subject of clear significance for vaccine design [27–29]. After uptake and processing of a protein antigen by B cells or dendritic cells, derived peptides are presented on the surface of the cell bound to MHC molecules in peptide-binding grooves. At this point, the folded structure of the original antigen appears irrelevant; nevertheless, it is well established that antibodies may be conformationally specific for the native or denatured forms of proteins [30–32]. Specificity for tertiary structure content may originate when intact antigens bind to their cognate immunoglobulins on the surface of B cells, which is a prerequisite for processing and presentation to T-helper cells, as well as stimulation of antibody release.

Previous investigations of the role of protein folding in antigenicity include a study of the immunogenicities of native versus heat-denatured ovalbumin [33], which found that the native protein was able to elicit an immune response in mice at 100-fold lower doses than the denatured protein. The resulting antisera generated were also specific for the native or denatured conformation used during immunization. The presence of antibodies directed to the denatured conformation of a protein is thought to be the cause of the often observed problem of nonneutralizing antibody responses, which nevertheless can be positive for the presence of antibody as measured by immunocapture techniques against plate-bound antigen [34]. Production of antibodies against the correct protein conformation is critical to the generation of a neutralizing antibody response [35–37].

The potential significance of mutationally induced alterations in folding stability of protein vaccines for immunogenicity deserves greater attention and bears further investigation in other model systems. Results presented in this study suggest that future vaccine design strategies directed toward antibody production may be optimized by carefully

considering the conformational stability of protein and most likely peptide antigens.

Acknowledgment

Spc. Shah Khan provided invaluable assistance to this work.

References

[1] P. Cleary, E. Kaplan, J. Handley, A. Wlazlo, M. Kim, A. Hauser, P. Schlievert, Clonal basis for resurgence of serious *Streptococcus pyogenes* disease in the 1980's, Lancet 339 (1992) 518–521.

[2] P. Schlievert, A. Assimacopoulos, P. Cleary, Severe invasive group A streptococcal disease: clinical description and mechanisms of pathogenesis, J. Lab. Clin. Med. 127 (1996) 13–22.

[3] M.H. Kim, P.M. Schlievert, Molecular genetics, structure, and immunobiology of streptococcal pyrogenic exotoxins A and C, in: D.Y. Leung, B.T. Huber, P.M. Schlievert (Eds.), Superantigens Molecular Biology, Immunology, and Relevance to Human Disease, Dekker, New York, 1997, pp. 257–279.

[4] D.L. Stevens, The flesh-eating bacterium: what's next? J. Infect. Dis. 179 (Suppl 2) (1999) S366–S374.

[5] M. Roggiani, J.A. Stoehr, S.B. Olmsted, Y.V. Matsuka, S. Pillai, D.H. Ohlendorf, P.M. Schlievert, Toxoids of streptococcal pyrogenic exotoxin A are protective in rabbit models of streptococcal toxic shock syndrome, Inf. Immunol. 68 (2000) 5011–5017.

[6] A.C. Papageorgiou, C.M. Collins, D.M. Gutman, J.B. Kline, S.M. O'Brien, H.S. Tranter, K.R. Acharya, Structural basis for the recognition of the superantigen streptococcal pyrogenic exotoxin A (SpeA1) by MHC class II molecules and T-cell receptors, EMBO J. 18 (1998) 9–21.

[7] J. Kline, C. Collins, Analysis of the superantigenic activity of mutant and allelic forms of streptococcal pyrogenic exotoxin A, Infect. Immun. 64 (1996) 861–869.

[8] J. Kline, C. Collins, Analysis of the interaction between the bacterial superantigen streptococcal pyrogenic exotoxin A (SpeA) and the human T-cell receptor, Mol. Microbiol. 24 (1997) 191–202.

[9] E. Sundberg, H Li, A. Llera, J. McCormick, J. Tormo, P. Schlievert, K. Karjalainen, R. Mariuzza, Structures of two streptococcal superantigens bound to TCR β chains reveal diversity in the architecture of T cell signaling complexes, Structure 10 (2002) 687–699.

[10] C.A. Earhart, G.M. Vath, M. Roggiani, P.M. Schlievert, D.H. Ohlendorf, Structure of streptococcal pyrogenic exotoxin A reveals a novel metal cluster, Prot. Sci. 9 (2000) 1847–1851.

[11] M. Baker, D. Gutmann, A. Papageorgiou, C. Collins, K. Acharya, Structural features of a zinc-binding site in the superantigen streptococcal pyrogenic exotoxin A (SpeA1): implications for MHC class II recognition, Prot. Sci. 10 (2001) 1268–1273.

[12] U.F. Hartwig, B. Fleischer, Mutations affecting MHC class II binding of the superantigen streptococcal erythrogenic toxin A, Int. Immunol. 5 (1993) 869–875.

[13] K. Nelson, P.M. Schlievert, R.K. Selander, J.M. Musser, Characterization and clonal distribution of four alleles of the speA gene encoding pyrogenic exotoxin A (scarlet fever toxin) in *Streptococcus pyogenes*, J. Exp. Med. 174 (1991) 1271–1274.

[14] M. Roggiani, J.A. Stoehr, B.A. Leonard, P.M. Schlievert, Analysis of toxicity of streptococcal pyrogenic exotoxin A mutants, Infect. Immun. 65 (1997) 2868–2875.

[15] P. Kraulis, MOLSCRIPT: a program to produce both detailed and schematic plots of protein structures, J. Appl. Crystallogr. 24 (1991) 946–950.

[16] S.C. Gill, P.H. von Hippel, Calculation of protein extinction coefficients from amino acid sequence data, Anal. Biochem. 182 (1989) 319–326.

[17] Y. Nozaki, The preparation of guanidine hydrochloride, Methods Enzymol. 26 (1972) 43–50.

[18] C. Pace, B. Shirley, J. Thomson, Measuring the conformational stability of a protein, in: T.E. Crieghton (Ed.), Protein Structure: A Practical Approach IRL Press, Oxford, 1989, pp. 311–330.

[19] G.P. Privalov, V. Kavina, E. Freire, P.L. Privalov, Precise scanning calorimeter for studying thermal properties of biological macromolecules in dilute solution, Anal. Biochem. 20 (1995) 79–85.

[20] G.H. Nabozny, J.M. Baisch, S. cheng, D. Cosgrove, M.M. Griffith, H.S. Luthra, C.S. David, HLA-DQ8 transgenic mice are highly susceptible to collagen-induced arthritis: a novel model for human polyarthritis, J. Exp. Med. 183 (1994) 27–37.

[21] R. LeClaire, S. Bavari, Human antibodies to bacterial superantigens and their ability to inhibit T-cell activation and lethality, Antimicrob. Agents Chemother. 45 (2001) 460–463.

[22] C. Pace, K. Shaw, Linear extrapolation method of analyzing solvent denaturation curves, Proteins Struct. Funct. Gen. 4 (Suppl 1) (2000) 1–7.

[23] M. Sundström, L. Abrahmsen, P. Antonsson, K. Mehindate, W. Mourad, M. Dohlsten, The crystal structure of staphylococcal enterotoxin type D reveals Zn^{2+}-mediated homodimerization, EMBO J. 15 (1996) 6832–6840.

[24] B. Welcher, J. Carra, R. Ulrich, L. DaSilva, C. David, M. Aman, S. Bavari, Lethal shock induced by streptococcal pyrogenic exotoxin A in mice transgenic for HLA-DQ8 and human CD4 receptors, J. Infect. Dis. 186 (2002) 501–510.

[25] R.G. Ulrich, S. Bavari, M.A. Olson, Staphylococcal enteroxins A and B share a common structural motif for binding class II major histocompatibility complex molecules, Nat. Struct. Biol. 2 (1995) 554–559.

[26] D. Grossman, M. Van, J.A. Mollick, S.K. Highlander, R.R. Rich, Mutation of the disulphide loop in staphylococcal enterotoxin A, J. Immunol. 147 (1991) 3274–3281.

[27] W. Laver, G. Air, R. Webster, S. Smith-Gill, Epitopes on protein antigens: misconceptions and realities, Cell 61 (1990) 553–556.

[28] S.J. Landry, Local protein instability predictive of helper T-cell epitopes, Immunol. Today 18 (1997) 527–532.

[29] L. Craig, P. Sanschagrin, A. Rozek, S. Lackie, L. Kuhn, L. Scott, The role of structure in antibody cross-reactivity between peptides and folded proteins, J. Mol. Biol. 281 (1998) 183–201.

[30] R.K. Brown, R. Delaney, L. Levine, H. van Vunakis, Studies on the antigenic structure of ribonuclease. I. General role of hydrogen and disulphide bonds, J. Biol. Chem. 234 (1959) 2043.

[31] D.C. Benjamin, J.A. Bersofsky, I.J. East, F.R.N. Gurd, C. Hannum, S.J. Leach, E. Margoliash, J.G. Michael, A. Miller, E.M. Prager, Reichlin E.E., Sercarz , S.J. Smith-Gill, P.E. Todd, A.C. Wilson, The antigenic structure of proteins: a reappraisal, Annu. Rev. Immunol. 2 (1984) 67–101.

[32] D.C. Benjamin, B-cell epitopes: fact and fiction, Adv. Exp. Med. Biol. 386 (1995) 95–108.

[33] C. Koch, S.S. Jensen, A. Oster, G. Houen, A comparison of the immunogenicity of the native and denatured forms of a protein, APMIS 104 (1996) 115–125.

[34] R. Jemmerson, Antigenicity and native structure of globular proteins: low frequency of peptide reactive antibodies, Proc. Natl. Acad. Sci. USA 84 (1987) 9180–9184.

[35] R.A. LaCasse, K.E. Follis, M. Trahey, J.D. Scarborough, D.R. Littman, J.H. Nunberg, Fusion-competent vaccines: broad neutralization of primary isolates of HIV, Science 283 (1999) 357–362.

[36] K.S. Steimer, C.J. Scandella, P.V. Skiles, N.L. Haigwood, Neutralization of divergent HIV-1 isolates by conformation-dependent human antibodies to Gp120, Science 254 (1991) 105–108.

[37] S. Subramanian, A. Karande, P. Adiga, Helix stabilization in the C-terminal peptide of chicken riboflavin carrier protein enhances immunogenicity and prolongs contraceptive potential as an epitope-based vaccine in female rats, Biochem. Biophys. Res. Commun. 287 (2001) 236–243.